Journal of Ethnopharmacology 272 (2021) 113951

Contents lists available at ScienceDirect

Journal of Ethnopharmacology

journal homepage: www.elsevier.com/locate/jethpharm

The chemical profiling of aqueous soluble fraction from *Lagopsis supina* and its diuretic effects *via* suppression of AQP and RAAS pathways in saline-loaded rats

Li Yang [a], Zhong-Wei He [b], Jun-Wei He [a,*]

[a] Jiangxi University of Traditional Chinese Medicine, Nanchang, 330004, China
[b] School of Information Technology, Jiangxi University of Finance and Economics, Nanchang, 330013, China

ARTICLE INFO

Keywords:
Lagopsis supina
LSB
Diuretic
Electrolytes
AQP
RAAS
Phytochemical constituents

ABSTRACT

Ethnopharmacological relevance: Lagopsis supina (Steph.) Ik. -Gal. ex Knorr. has been widely used as a remedy treatment for diuresis and edema in China over 2500 years. Our previous results showed that the aqueous soluble fraction from *L. supina* (LSB) possessed acute diuretic effect.

Aim of the study: The aim of this study was to appraise the acute (6 h) and prolonged (7 d) diuretic effects, underlying mechanisms, and chemical profiling of LSB.

Materials and methods: The chemical profiling of LSB was performed by ultra-high-performance liquid chromatography-quadrupole time-of-flight tandem mass spectrometry (UHPLC-qTOF-MS/MS). Then, oral administration of LSB (40, 80, 160 and 320 mg/kg) and furosemide (10 mg/kg) once daily for 7 consecutive days to evaluate the diuretic effects in saline-loaded rats. The body weight, food consumption, and water intake were recorded once daily. The urinary volume, pH and electrolyte concentrations (Na^+, K^+, Cl^-, and Ca^{2+}) were measured after administration drugs for acute and prolonged diuretic effects. In addition, the serum levels of Na^+-K^+-ATPase, angiotensin II (Ang II), anti-diuretic hormone (ADH), aldosterone (ALD), atriopeptin (ANP), aquaporins (AQPs)-1, 2 and 3 were determined by ELISA kits. The mRNA expressions and protein levels of AQPs-1, 2 and 3 were analyzed by real-time quantitative PCR and Western blot assays, respectively.

Results: 30 compounds were identified in LSB based on accurate mass and MS/MS fragmentation compared to literature, among which phenylpropanoids and flavonoids could be partly responsible for the major diuretic effect. Daily administration of LSB (160 or 320 mg/kg) prominently increased urinary excretion volume after the 2 h at the first day of treatment, remaining until the 7th day. LSB did not cause Na^+ and K^+ electrolyte abnormalities, and has minor effect on Cl^- and Ca^{2+} concentrations at 320 mg/kg. Furthermore, LSB observably suppressed renin-angiotensin-aldosterone system (RAAS) activation, including decreased serum levels of Ang II, ADH, and ALD, and prominently increased serum level of ANP in rats. LSB treatment significantly down-regulated the serum levels, mRNA expressions and protein levels of AQP1, AQP2, and AQP3.

Conclusion: LSB has a prominent acute and prolonged diuretic effects *via* suppression of AQP and RAAS pathways in saline-loaded rats, and support the traditional folk use of this plant. Taken together, LSB might be a potential diuretic agent.

1. Introduction

Diuretic agents have been widely used to treat edema caused by various pathological progress by acting on the kidney, which play a pivotal role regulating urinary volume and electrolyte excretions (Cechinel-Zanchett et al., 2020; Li et al., 2020). Consequently, diuretic

Abbreviations: LSB, the aqueous soluble fraction from *Lagopsis supina*; UHPLC-qTOF-MS/MS, ultra-high-performance liquid chromatography-quadrupole time-of-flight tandem mass spectrometry; ESI, electrospray ionization; Ang II, angiotensin II; ADH, anti-diuretic hormone; ALD, aldosterone; ANP, atriopeptin; AQP, aquaporin; ELISA, enzyme-linked immunosorbent assay; RAAS, renin-angiotensin-aldosterone system; TCMs, traditional Chinese medicines; EtOH, ethanol; FUR, furosemide; SD, standard deviation; ANOVA, analysis of variance.

* Corresponding author.
E-mail addresses: yangli07971@163.com (L. Yang), 39732505@qq.com (Z.-W. He), hjwjn2008@163.com (J.-W. He).

https://doi.org/10.1016/j.jep.2021.113951
Received 15 September 2020; Received in revised form 11 December 2020; Accepted 16 February 2021
Available online 18 February 2021

Table 1
Primer sequences used for qRT-PCR.

Gene	Sequence 5'→3'	
	Forward	Reverse
AQP1	ATTGCAGCGTCATGTCTGAG	GAACTAGGGGCATCCAAAC-3
AQP2	TTGCAGGAACCAGACACTTG	GCGGAGACGAGCACTTTTAC
AQP3	ACTCCAGTGTGGAGGTGGAC	GCCCCTAGTTGAGGATCACA
GAPDH	TGATTCTACCCACGGCAAGTT	TGATGGGTTTCCCATTGATGA

therapy remains the cornerstone of treatment, and diuretic agents as the gold standard and first-line option drugs for the treatment of edema, hypertension, congestive heart failure, malignant ascites effusion, stroke, cardiovascular diseases, and other kidney diseases (Cechinel-Zanchett et al., 2020; Li et al., 2020; Lou et al., 2018; Younis et al., 2020). Nevertheless, conventional diuretic agents, for instance loop diuretics and thiazide diuretics, long-term use can cause some serious adverse effects, such as electrolyte disturbances, hypercalcemia, hyperglycemia, arrhythmia (Cechinel-Zanchett et al., 2020; Li et al., 2020; Younis et al., 2020). As a result of this, exploring effective and safe diuretic candidates from natural products, especially traditional folk medicines, could be a momentous breakthrough.

In this context, traditional Chinese medicines (TCMs) abundant in bio-constituents are a promising natural alternative, and have been verified to be effective in treating diuresis for centuries with more safer and little side-effects in China and other Southeast Asian countries (Liu et al., 2019a; Yang et al., 2020a, b, c; Yang and He, 2019, 2021). From this perspective, *Lagopsis supina* (Steph.) Ik. -Gal. ex Knorr., locally known as Xiazhicao (夏至草), is native to China, and has been used for centuries as an empiric diuretic agent to treating kidney diseases (He et al., 2019a, 2020). Despite good clinical practice and great clinical effects of *L. supina*, no study has demonstrated its traditional use as diuretic activity yet. Previously, we investigated the acute diuretic activity of the crude ethanol extract and its four fractions (LSA~D) from *L. supina* in saline-loaded rats, and LSB exhibited remarkably diuretic effects (Liu et al., 2019a). However, the prolonged diuretic effect (7 d), underlying mechanism, and phytochemical profiling of LSB are still unknown yet, leading to numerous obstacles in the clinical application and reasonable development of *L. supina*.

To systematically study LSB, in this work, the saline-loaded rat model was adopted to evaluate the acute and prolonged diuretic effects, and underlying molecular mechanisms of LSB. Following this step, ultra-high-performance liquid chromatography-quadrupole time-of-flight tandem mass spectrometry (UHPLC-qTOF-MS/MS) analysis was performed to identify the phytochemical constituents present in this fraction. Our findings will provide potential scientific evidence for the development and clinical application of *L. supina*.

2. Materials and methods

2.1. Chemicals and drugs

Ethanol (EtOH) and petroleum ether were purchased from Sinopharm Chemical Reagent Co., Ltd. (Shanghai, China). LC-MS grade acetonitrile was provided by Fisher Scientific (Pittsburgh, USA). Deionized water was purified by a Milli-Q water system (Merk Millipore, Milford, USA). Pentobarbital sodium (rb-02221) was purchased from Shanghai Rongbai Biological Technology Co., Ltd. (Shanghai, China). All other agents used were of the analytical reagent grade.

Furosemide (a reference loop diuretic drug) was obtained from Jiangsu Yabang Aipusen Pharmaceutical Co., Ltd. (Jiangsu, China).

2.2. Plant collection, extraction and fractionation

The whole plants of L. supina (number XZC201606) were collected from Inner Mongolia University for Nationalities (GPS location: 43.62500302788547,122.25993999999997), Inner Mongolia, China, deposited at our lab, and authenticated by professor Guoyue Zhong at Jiangxi University of Traditional Chinese Medicine. The air-dried and powdered plant materials (38.0 kg) were extracted with 95% EtOH (300 L × 3) and subsequently 50% EtOH (300 L × 3) by maceration at room temperature for 7 days. All filtrates were combined and evaporated under reduced pressure to obtain the ethanol crude extract of L. supina (LS, 8.7 kg), which was suspended in water and partitioned successively with petroleum ether to afford petroleum ether portion (LSA) and water portion. Then, the water portion was subjected to a chromatographed on a D101 macroporous resin column using a gradient solvent of aqueous ethanol (0%, 30%, 60% and 95%) to obtain five fractions: 0% (LSB), 30% (LSC, 669.0 g), 60% (LSD), and 95% (LSE, merged with LSA based on the thin layer chromatography analysis).

2.3. Phytochemical profile

Phytochemical analysis of LSB was carried out using UHPLC-qTOF-MS/MS on a Shimadzu UHPLC System (Kyoto, Japan) coupled with an AB SCIEX Triple TOFTM 5600+ system (Foster City, CA, USA) (Yang et al., 2019). The MS was performed by electrospray ionization (ESI) source in negative-ion mode. The following parameters were used: capillary voltage, 5.5 kV; drying temperature, 500 °C; nebulizer pressure, 50 psi. The analysis was carried out 100–1500 Da of mass ranges. Chromatographic separation was conducted on a Luna Omega C18 (100 × 2.1 mm, 1.6 μm, Phenomenex Inc., CA, USA) keeping at 40 °C. 0.1% aqueous formic acid (v/v, A) and acetonitrile (B) were used as mobile phases. The gradient elution with the flow rate of 0.3 mL/min was performed as follows: 0–10 min 5–5% B; 10–35 min 5–25% B; 35–45 min 25–95% B; 45–50 min 95–95% B; 50.1–53 min 5–5% B. The sample

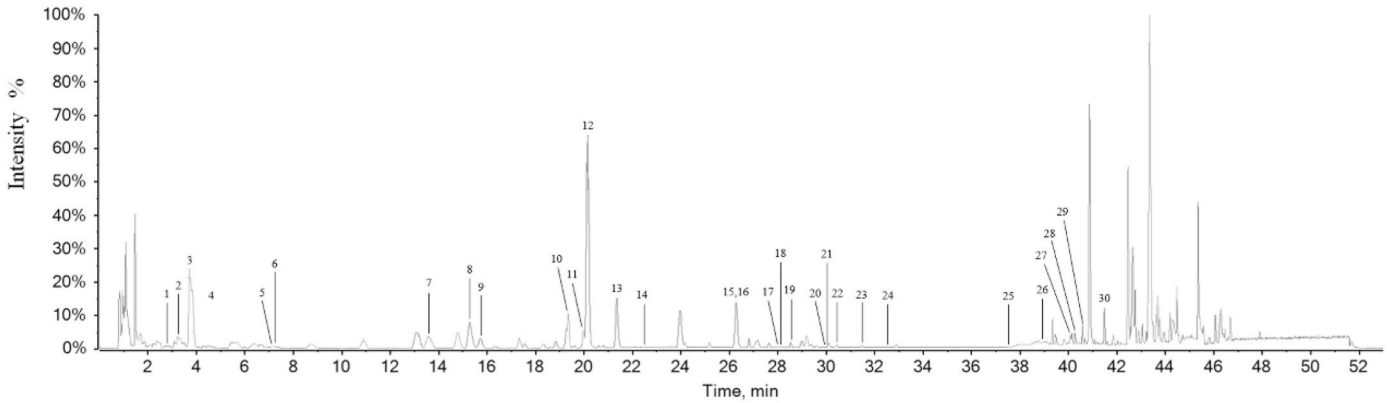

Fig. 1. The base peak chromatogram of LSB by UHPLC-qTOF-MS/MS in negative-ion mode. The peak numbers are consistent with those reported in Table 1.

Table 2
Chemical constituents identified from LSB by UHPLC-qTOF-MS/MS in negative-ion mode.

Peak	RT (min)	Compound	Molecular Formula	Molecular Weight	Measured Mass [M - H]$^-$	Error (ppm)	MS^2	Reference
1	2.80	Antirrinoside	$C_{15}H_{22}O_{10}$	362.1213	361.11402	−2.1	253.0217, 181.0436, 153.0581,71.0262, 59.0322	-[a]
2	3.28	1-*O*-Caffeoyl-*β*-D-glucopyranose	$C_{15}H_{18}O_9$	342.09508	341.08781	−2.4	341.0872, 179.0348, 161.0252, 135.0467, 133.0309	Jiménez-Sánchez et al. (2016)
3	3.76	Harpagide	$C_{15}H_{24}O_{10}$	364.13695	363.12967	−2.2	207.0657, 201.0765, 183.0675, 165.0575,139.0420, 125.0272, 99.0128, 97.0333, 89.0284, 59.0193	Wu et al. (2017)
4	4.66	Geniposidic acid	$C_{16}H_{22}O_{10}$	374.1213	373.11402	−2.1	211.0699,167.0670, 149.0626, 123.0484, 119.0489, 89.0300, 59.0198	Zhou et al. (2020)
5	7.06	Mussaenosidic acid	$C_{16}H_{24}O_{10}$	376.13695	375.12967	−3.8	375.1319, 213.0787, 169.0883, 151.0789, 125.0619, 107.0580, 89.0311, 59.0260	Zhou et al. (2020)
6	7.19	Decaffeoylacteoside	$C_{20}H_{30}O_{12}$	462.17373	461.16645	−4.8	461.1605, 315.1057, 161.0442, 135.0451, 113.0280	Zhou et al. (2020)
7	13.77	6,7-Dihydroxycoumarin	$C_9H_6O_4$	178.02661	177.01933	4.3	177.0199, 133.0290,105.0358,93.0381,89.0452,77.0449	He et al. (2019)
8	15.29	Chlorogenic acid	$C_{16}H_{18}O_9$	354.09508	353.08781	−1.1	191.0571	Jiménez-Sánchez et al. (2016)
9	15.74	Methyl 2-*O*-*β*-D-glucopyranosylbenzoate	$C_{14}H_{18}O_8$	314.10017	313.09289	−1.0	269.1029, 167.0360, 152.0122, 123.0473, 108.0239	-[a]
10	19.35	8-*O*-Acetylharpagide	$C_{17}H_{26}O_{11}$	406.14751	405.14024	−3.7	207.0720, 183.0650, 165.0565, 139.040426, 121.0315, 89.0282, 85.0342, 71.0222, 59.0209	Wu et al. (2017)
11	20.07	3-*p*-Coumaroylquinic acid	$C_{16}H_{18}O_8$	338.10017	337.09289	−0.2	337.0497, 191.0577, 163.0418, 119.0516, 93.0377	Liu et al. (2019b)
12	20.15	Caffeic acid	$C_9H_8O_4$	180.04226	179.03498	3.8	135.0472, 134.0392, 117.0374, 107.0531, 89.0459, 79.0624	Zhou et al. (2020)
13	21.35	Syringic acid	$C_9H_{10}O_5$	198.05282	197.04555	4.4	182.0257,166.9996, 138.0342, 123.0115, 121.0322,106.0095,78.0173	Angeloni et al. (2020)
14	22.43	Methyl 4-caffeoylquinate	$C_{17}H_{20}O_9$	368.11073	367.10346	−2.1	193.0508, 191.0560, 134.0380, 93.0381	Liu et al. (2019b)
15	26.29	Ferulic Acid	$C_{10}H_{10}O_4$	194.05791	193.05063	5.0	178.0291, 134.0392, 133.0317, 117.0381, 89.0445	Zhang et al. (2016)
16	26.41	Rutin	$C_{27}H_{30}O_{16}$	610.15339	609.14611	−2.2	609.1415, 300.0233	Yang and He (2020)
17	28.02	Stachysoside A	$C_{34}H_{44}O_{19}$	756.24768	755.2404	−2.8	755.2386, 593.2052, 161.0265	Yang and He (2020)
18	28.17	Quercetin-3-*O*-*β*-D-glucoside	$C_{21}H_{20}O_{12}$	464.09548	463.0882	−3.4	463.0876, 301.0337, 300.0251,271.0272	Yang and He (2020)
19	28.53	Acteoside	$C_{29}H_{36}O_{15}$	624.20542	623.19814	−3.6	623.1972,461.1640, 315.1049, 179.0357, 161.0256, 135.0454	Zhou et al. (2020)
20	29.82	Luteolin-7-*O*-*β*-D-glucoside	$C_{21}H_{20}O_{11}$	448.10056	447.09329	−4.2	331.0827, 287.0890, 269.0816, 243.1031	Liu et al. (2019c)
21	30.08	Quercetin-3-*O*-6-(3-hydroxy-3-methylglutaryl)-*β*-D-glucoside	$C_{27}H_{28}O_{16}$	608.13774	607.13046	−3.6	607.1263, 545.1278, 505.0897, 463.0854, 301.0317,300.0275	-[a]
22	30.53	Jionoside B1/B2	$C_{37}H_{50}O_{20}$	814.28954	813.28227	−2.4	813.2842, 637.2371, 491.1851, 175.0412	Yang and He (2020)
23	31.30	Apigenin-7-*O*-*β*-D-glucoside	$C_{21}H_{20}O_{10}$	432.10565	431.09837	−3.1	431.0980, 311.0548, 269.0451, 268.0372	Liu et al. (2019c)
24	32.32	3,5-di-*O*-caffeoylquinic acid	$C_{25}H_{24}O_{12}$	516.12678	515.1195	−2.3	515.1219, 353.0866, 191.0599,179.0349,173.0454	Yang and He (2020)
25	37.49	Luteolin	$C_{15}H_{10}O_6$	286.04774	285.04046	1.4	285.0310, 244.9847,241.0479, 216.9895, 200.8664, 178.9947, 151.0039, 149.0230, 133.0317, 132.0219	Yang and He (2020)
26	38.96	Apegenin	$C_{15}H_{10}O_5$	270.05282	269.04555	−0.1	269.0456,228.9886, 154.9921, 117.0354	Yang and He (2020)
27	40.12	Hydroxygenkwanin	$C_{16}H_{12}O_6$	300.06339	299.05611	−0.3	298.9953, 284.0327, 278.9859, 232.9823, 228.9857, 116.9963	-[a]
28	40.37	Leoheterin	$C_{20}H_{30}O_4$	334.21441	333.20713	−0.8	333.9851,272.9941, 266.9862, 252.9897,244.9837, 228.9917, 216.9874, 178.9930, 140.9959,69.0030	-[a]
29	40.59	Apigenin-7-*O*-(3″,6″-di-(*E*)-*p*-coumaroyl)-*β*-D-galactopyranoside	$C_{39}H_{32}O_{14}$	724.17921	723.17193	−0.8	723.1699, 559.1248, 453.1169, 269.0461, 145.0309	-[a]
30	41.35	Lagopsin C	$C_{22}H_{36}O_6$	396.25119	395.24391	−2.5	374.9905, 354.9804, 334.9818, 314.9876, 306.9827, 240.9902, 228.9994, 154.9935, 59.0277	-[a]

a No reference.

inject volume was 3 μL.

2.4. Animals

Male Sprague-Dawley rats (Certificate no. SCXK (su) 2007–0008, 180–220 g) were purchased from Nanjing Qinglongshan animal berrding farm (Nanjing, China), and were kept in a temperature- and light-controlled room (21–25 °C; 12 h light/dark cycle) with free access to food and water. All animal procedures were approved by the institutional animal care and use committee of Jiangxi University of

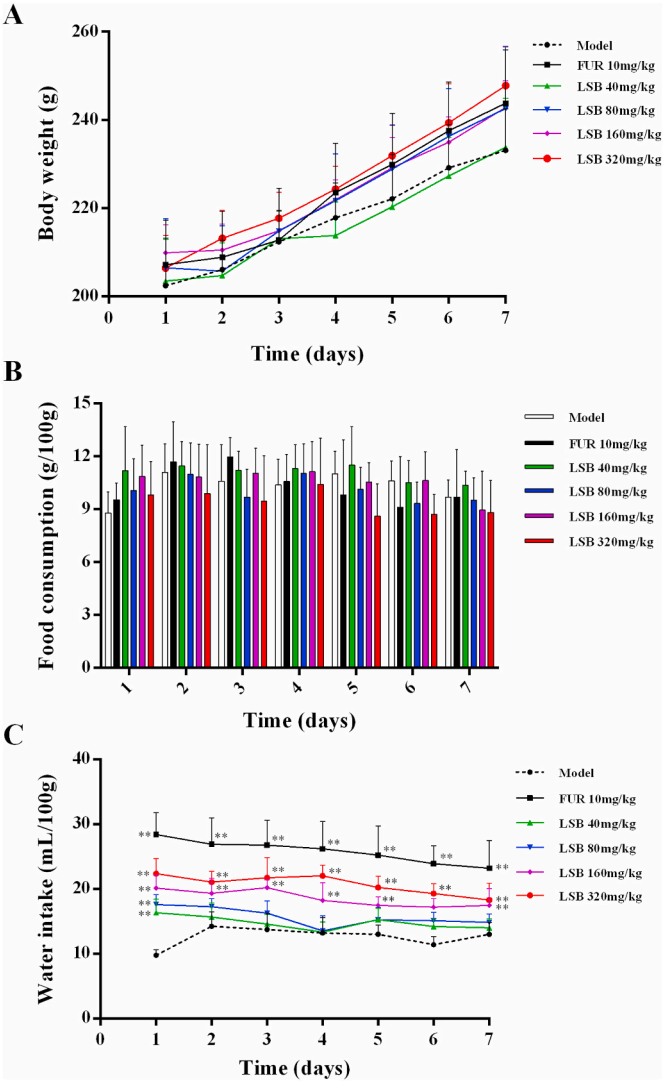

Fig. 2. Effect of LSB on the body weight (A), food consumption (B), and water intake (C) in saline-loaded rats. Data are shown as mean ± SD (n = 8). $^{**}p < 0.01$ compared with the model group using ANOVA followed by the Dunnett's test.

Traditional Chinese Medicine.

2.5. Assessment of diuretic activity

2.5.1. Experimental design

After adaptive feeding, all rats were fasted for 12 h before the test with water ad libitum. Each rat was housed individually in a metabolic cage for three days adapatation. The diuretic activity was performed according to the method described in our previous paper (Liu et al., 2019a).

2.5.2. Acute diuretic activity

Before treatment for 30 min, all rats were received by gavage 5 mL/100g body weight of physiological saline solution in order to impose water and solidum body uniformity (Liu et al., 2019a). Then, the 48 rats were randomly distributed into 6 groups (n = 8). In sequence, they were orally treated by gavage with 10 mL/kg of water (Model group, saline-loaded rats), 10 mg/kg of furosemide (FUR group), or LSB groups (40, 80, 160, or 320 mg/kg of LSB). Each rat was housed individually in a metabolic cage, and the cumulative urinary output volume was measured at 1, 2, 4, and 6 h of day 1 after administration, which were expressed as mL/100 g. Urinary pH values and electrolyte concentrations (Na^+, K^+, Cl^-, and Ca^{2+}) were measured within the 6 h urine samples of all rats.

2.5.3. Prolonged diuretic activity

In this set experiment, all group rats were administered orally once a day from day 1 to day 7 when saline-loaded rats were established as the same as above, and the body weight, food consumption, and water intake, as well as cumulative urinary excretion volume, pH, and electrolyte concentrations (Na^+, K^+, Cl^-, and Ca^{2+}) were recorded every 24 h. Furthermore, the daily food consumption, water intake and cumulative urinary excretion were expressed as g/100 g and mL/100 g, respectively. On the 7th day after administration, all rats were killed after anesthesia (1% pentobarbital sodium, 40 mg/kg), and the blood samples and kidney tissues were harvested (Liu et al., 2019a). The blood sample (7 mL) was collected from the artery of rat, and subsequently subjected to centrifugation (2500 rpm for 15 min at 4 °C). The urine and serum, and kidney tissues were stored at −20 and −80 °C for further analysis, respectively.

2.5.4. Biochemical methods

The urinary pH value was measured using a PHS-3E pH meter (Shanghai Inesa Scientific Instrument Co., Ltd., Shanghai, China). The urinary Na^+, K^+, Cl^-, and Ca^{2+} concentrations were determined using commercial reagent kits (Nanjing JianCheng Institute of Biotechnology Co., Ltd., Nanjing, China). The Na^+-K^+-ATPase activity, as well as Ang II, ANP, ADH, ALD, AQP1, AQP2, and AQP3 levels in serum were determined using commercial ELISA kits (Chuzhou Shinuoda Biological Technology Co., Ltd., Chuzhou, China), which were performed by the manufacture's instructions.

2.5.5. RNA-isolation and RT-PCR

Renal samples were homogenized and extracted with TRizol (l ml/100 mg, Invitrogen Life Technologies, USA) to obtain the total RNAs. The concentration and purity of total RNAs were measured by Nanodrop 2000 (Thermo Fisher Scientific, Waltham, USA). The cDNA was synthesized according to the PrimeScript RT Reagent Kit with gDNA Eraser protocol (Perfect Real Time, TaKaRa bio. Inc. Dalian, China). The primer sequences were used to amplify specific cDNA fragments shown in Table 1. All qRT-PCR reactions were performed in 20 μl reactions of SYBR qPCR mix (TaKaRa bio. Inc. Dalian, China) containing 2.0 μl cDNA, 0.8 μl of each of the forward and reverse primers, 7.0 μl 2 × SYBR Green qPCR Mix, 0.4 μl Rox Reference Dye (50 ×) and 9.0 μl dd H_2O. The following thermal profile for the Real-time PCR assays was used: 2 min at 95 °C (first segment, one cycle), followed by denaturation for 15 s at 95 °C, annealing for 34 s at 60 °C (second segment, 40 cycle), and elongation for 30 s at 72 °C with the acquisition of fluorescent data using a StepOnePlus Real-Time PCR Systems (Thermo Fisher Scientific, Waltham, USA). The relative gene expression level was calculated using the $2^{-\Delta\Delta CT}$ method, with GAPDH as the internal control.

2.5.6. Western blot analysis

The kidney tissues were harvested from rats, and the method of Western blot analysis was provided in our previous paper (He et al., 2019a). The primary antibodies of AQP1 (1:2000, Abcam, Cambridge, UK), AQP2 (1:1000, CST, Boston, USA) and AQP3 (1:1000, Abcam, Cambridge, UK), and the secondary antibodies of horseradish peroxidase-conjugated (1:5000, Abcam, Cambridge, UK) were used in this experiment. GAPDH was used as a reference protein.

2.6. Data processing

Graphpad Prism6 was used for statistical analysis, and the data were presented as the means ± standard deviation (SD). One-way analysis of variance (ANOVA) and the Dunnett's test were used for comparison model and treated groups. The Mann-Whitney *U* test was also used for

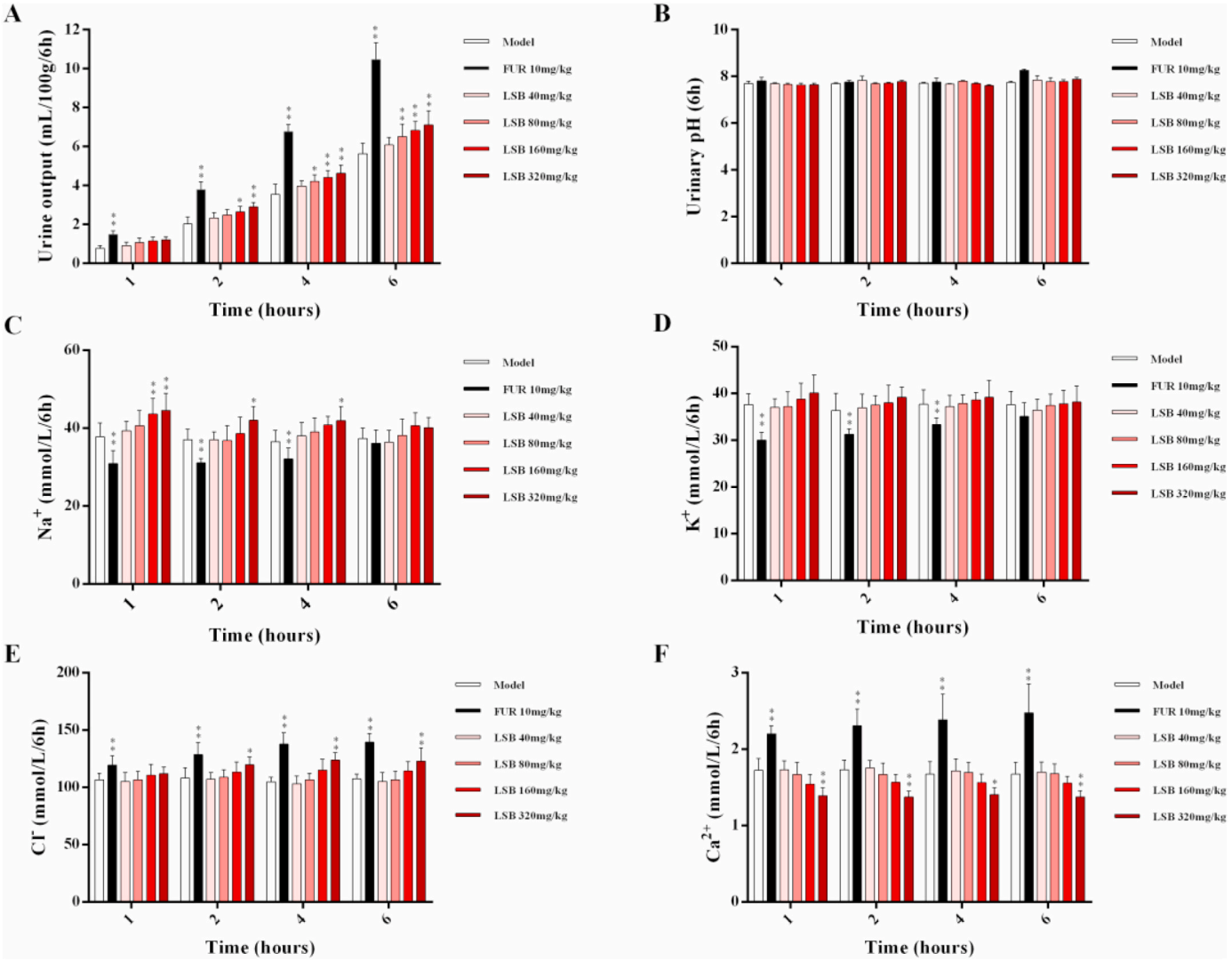

Fig. 3. Acute diuretic effects of LSB on urine output volume (A), urinary pH (B), urinary Na^+ concentration (C), urinary K^+ concentration (D), urinary Cl^- concentration (E), and urinary Ca^{2+} concentration (F) in saline-loaded rats. Data are shown as mean ± SD (n = 8). *$p < 0.05$ and **$p < 0.01$ compared with the model group using ANOVA followed by the Dunnett's test.

comparison differences groups of genes expression levels. Differences with $P < 0.05$ indicated statistical significance.

3. Results

3.1. Phytochemical investigation of LSB

The chemical constituents corresponding to the chromatographic peaks in LSB (Fig. 1) were determined by MS/MS analysis using negative-ion mode based on their accurate mass, and fragment ions in comparison with those of data reported in literature.

As a result, a total of 30 compounds, including 11 phenylpropanoids (peaks 2, 7, 8, 11, 12, 14, 15, 17, 19, 22, and 24), 9 flavonoids (peaks 16, 18, 20, 21, 23, 25–27, and 29), 5 monoterpenoids (peaks 1, 3–5, and 10), 2 diterpenoids (peaks 28 and 30), and 3 others (peaks 6, 9, and 13) were identified from LSB based on UHPLC-qTOF-MS/MS (Table 2).

Take peak 19 as an example, it had $[M-H]^-$ ion at *m/z* 623.1972, and MS^2 spectrum showed the fragment ions at *m/z* 461.1640 [M-H-caffeoyl]$^-$, *m/z* 315.1049 [M-H-caffeoyl-$C_6H_{10}O_4$]$^-$, *m/z* 179.0357 [caffeic acid-H]$^-$, 161.0256 [caffeic acid-H-H_2O]$^-$ and 135.0454 [M-H-caffeoyl-$C_6H_{10}O_4$-Glc-H_2O]$^-$. Compared with literature data, the peak 19 was identified as acteoside (Yang and He, 2020). Furthermore, the flavonoid aglycones were easily cleavable through the Retro-Diels-Alder (RDA) reaction at the 1,3-bonds of the C ring under negative ion mode to produce a character-istic fragment ion m/z *151* $[^{1,3}A]^-$, and the number increasing of hydroxyl groups on the B and C rings obtained fragment ions with difference of 16 Da such as *m/z* 133 $[^{1,3}B]^-$ (Luteolin, peak 25) and *m/z* 117 $[^{1,3}B]^-$ (Apigenin, peak 26). In addition, all flavonoid aglycones easily lose neutral molecules such as CO_2, C_2H_2O, C_3O_2, H_2O in negative ion mode, and get fragment ions of 44, 42, 68, and 18 Da, respectively (Yang et al., 2019).

3.2. Effect of LSB on body weight, food consumption, and water intake

The body weight, food consumption, and water intake of all rats under this experiment were evaluated at every day from day 1 to day 7. As shown in Fig. 2, the body weight and food consumption of LSB and furosemide groups did not show pronounced differences when in comparison with the model group ($p > 0.05$). In addition, the volumes of water intake after treatment with LSB (160 or 320 mg/kg) or furosemide (10 mg/kg) were significantly increased ($p < 0.01$) when compared to the model group every day, as expected.

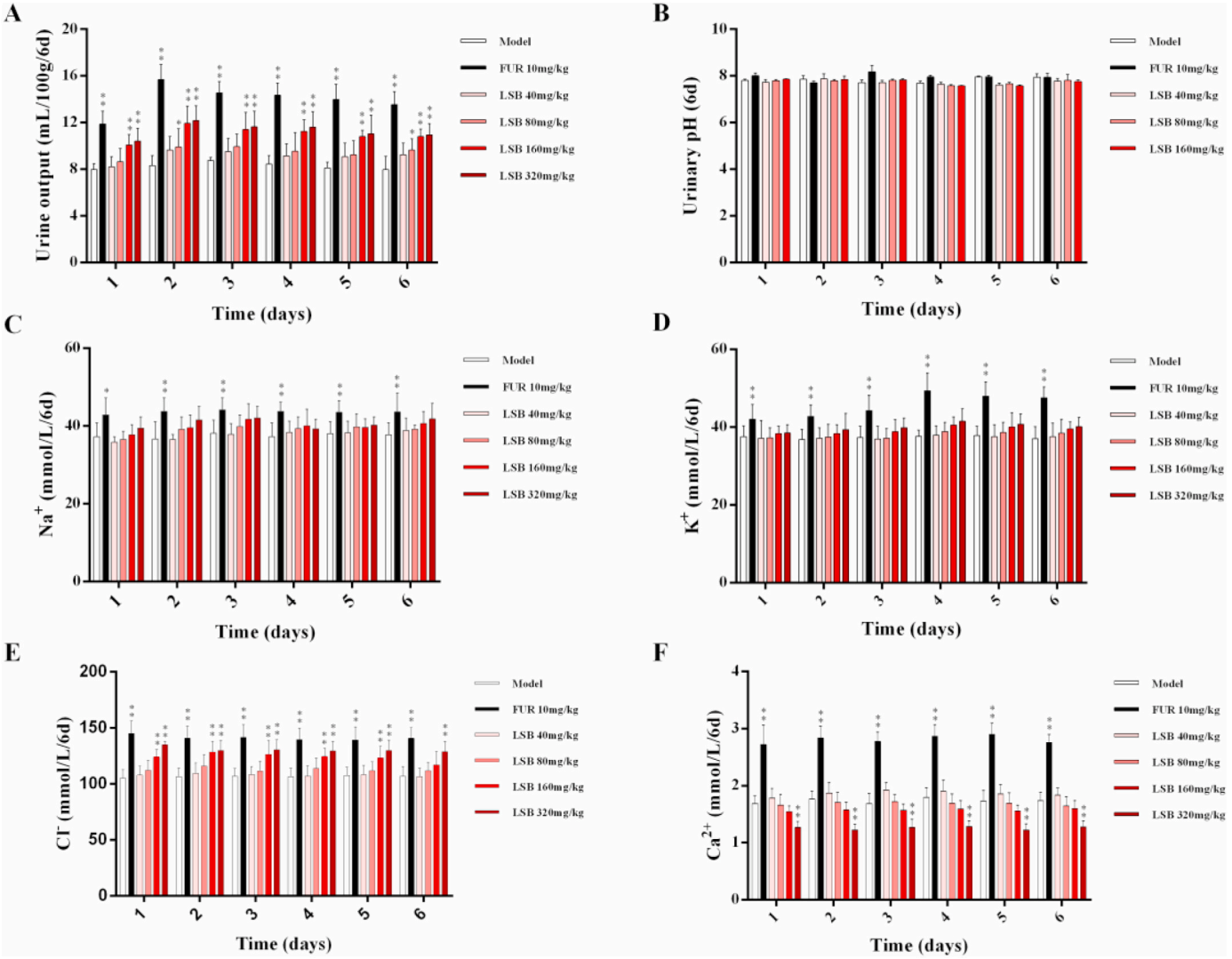

Fig. 4. Prolonged diuretic effects of LSB on urine output volume (A), urinary pH (B), urinary Na^+ concentration (C), urinary K^+ concentration (D), urinary Cl^- concentration (E), and urinary Ca^{2+} concentration (F) in saline-loaded rats. Data are shown as mean ± SD (n = 8). *$p < 0.05$ and **$p < 0.01$ compared with the model group using ANOVA followed by the Dunnett's test.

3.3. Acute diuretic activity of LSB

3.3.1. LSB increased urinary excretion volume

To determine whether LSB has acute diuretic activity, we recorded urinary excretion volume in saline-loaded rats after oral administration of LSB at four dosages of 40, 80, 160 and 320 mg/kg within 6 h for the first day treatment. As presented in Fig. 3A, compared to the model group, the cumulative urinary excretion volumes obviously increased in rats treated with LSB (160 or 320 mg/kg) after the 2–6 h at the first day ($p < 0.05$ or $p < 0.01$), whereas, not as strong as furosemide ($p < 0.01$), a classical high loop diuretic agent. Additionally, oral administration of 80 mg/kg LSB also significantly enhance urinary excretions after 4–6 h at the first day of treatment ($p < 0.05$ or $p < 0.01$). Thus, in summary, results obtained by four different dosages of LSB have shown that there were a parallel enlarge of urinary output volume as the dosage increased, demonstrating that the diuretic effects of LSB possessed a dose-dependent behavior.

3.3.2. LSB does not affect urinary pH

The treatment with LSB (40–320 mg/kg) or furosemide (10 mg/kg) have not been able to change the pH values after 6 h at the first day in comparison with the model group (Fig. 3B).

3.3.3. LSB resulted in less urinary electrolyte disorder than furosemide

As summarized in Fig. 3, the positive control group of furosemide (10 mg/kg) exhibited prominent decreased in Na^+ (Fig. 3C) and K^+ (Fig. 3D) excretions, and remarkable increased in Cl^- (Fig. 3E) and Ca^{2+} (Fig. 3F) excretion in 6 h at the first day when compared to the model group. In contrast to the furosemide, LSB is a potential acute diuretic drug by reducing less electrolytes disorder.

3.4. Prolonged diuretic activity

3.4.1. LSB increased urinary excretion volume

To determine whether LSB has prolonged diuretic activity, we measured urinary excretion volumes in rats for 6 consecutive days (Fig. 4A). Comparted with the model group, the urinary excretion volumes were remarkably increased from day 1 to day 6 after treatment with 10 mg/kg furosemide, 160 and 320 mg/kg LSB ($p < 0.01$). In addition, the prolonged diuretic effects of LSB also possessed a dose-dependent behavior in this experiment.

3.4.2. LSB does not affect urinary pH

The urinary pH values were also not affected by any of the LSB or furosemide tested in the prolonged diuretic activity experiments

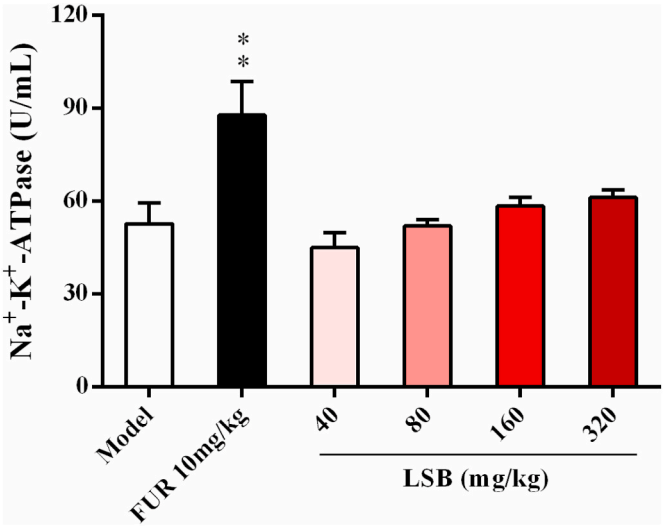

Fig. 5. Effect of LSB on serum Na^+-K^+-ATPase activity in saline-loaded rats. Data are shown as mean ± SD (n = 8). $^{**}p < 0.01$ compared with the model group using ANOVA followed by the Dunnett's test.

(Fig. 4B, $p > 0.05$).

3.4.3. LSB resulted in less urinary electrolyte disorder than furosemide

As expected, there were observably up-regulated in all urinary electrolyte excretions, including Na^+ (Fig. 4C), K^+ (Fig. 4D), Cl^- (Fig. 4E) and Ca^{2+} (Fig. 4F) excretion after treatment furosemide (10 mg/kg) from day 1 to day 6 when compared with those of the model group ($p < 0.01$). In contrast to the positive control of furosemide group, all four dosages of LSB did not affected the urinary Na^+ and K^+ concentrations when compared to the control group. Meanwhile, only higher LSB dosages (160 and 320 mg/kg) notably increased the urinary Cl^- concentrations in comparison to the model group. Additionally, only 320 mg/kg LSB significantly decreased the urinary Ca^{2+} concentration.

3.4.4. LSB less increased serum Na^+-K^+-ATPase activity than furosemide

Furthermore, in order to further understand the effects on electrolyte excretions after LSB-treated in saline-loaded rats, the serum Na^+-K^+-ATPase activity was also determined. As illustrated in Fig. 5, the treatment with LSB (40–320 mg/kg) did not changed the serum Na^+-K^+-ATPase activity, as expected, but less increased than furosemide ($p < 0.01$).

3.5. Evaluation of underlying mechanisms involved in the diuretic activity

3.5.1. Effect of LSB on serum levels of Ang II, ADH, ALD, and ANP

To explore whether LSB takes part in renin-angiotensin-aldosterone system (RAAS), we measured the serum levels of Ang II, ADH, and ALD in rats. Daily oral administration of LSB (80, 160, or 320 mg/kg) prominently decreased the rat serum levels of Ang II, ADH, and ALD ($p < 0.01$, Fig. 6A–C), whereas, only decreased ADH level after treatment with furosemide when in comparison to those of the model group ($p < 0.01$). Subsequently, the ANP serum level in rats was also recorded, and only 80–320 mg/kg LSB remarkably enhanced the contents compared to that of the model group ($p < 0.01$, Fig. 6D). The results suggested that LSB suppressed the RAAS and the release of ANP, whereas, the positive

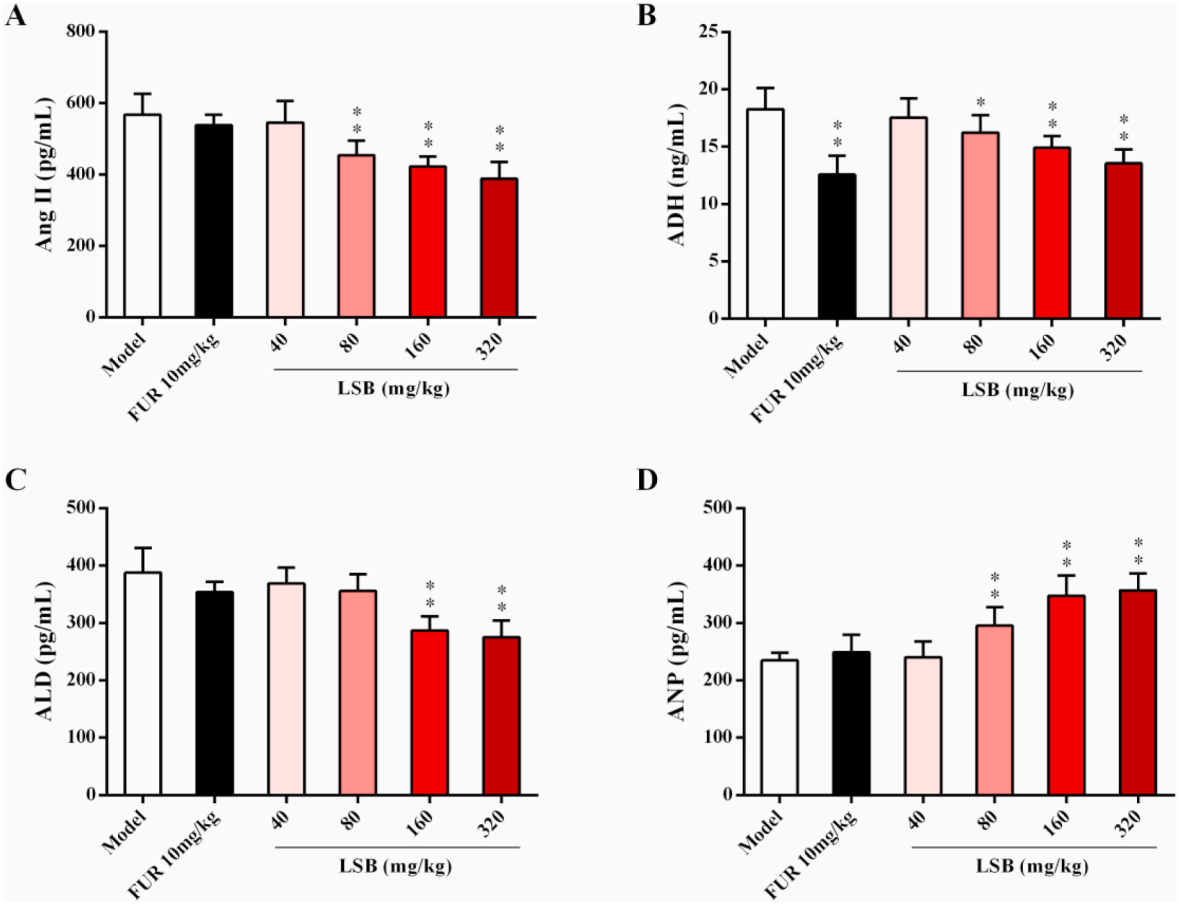

Fig. 6. Effect of LSB on serum levels of Ang II (A), ADH (B), ALD (C), and ANP (D) in saline-loaded rats. Data are shown as mean ± SD (n = 8). $^{*}p < 0.05$ and $^{**}p < 0.01$ compared with the model group using ANOVA followed by the Dunnett's test.

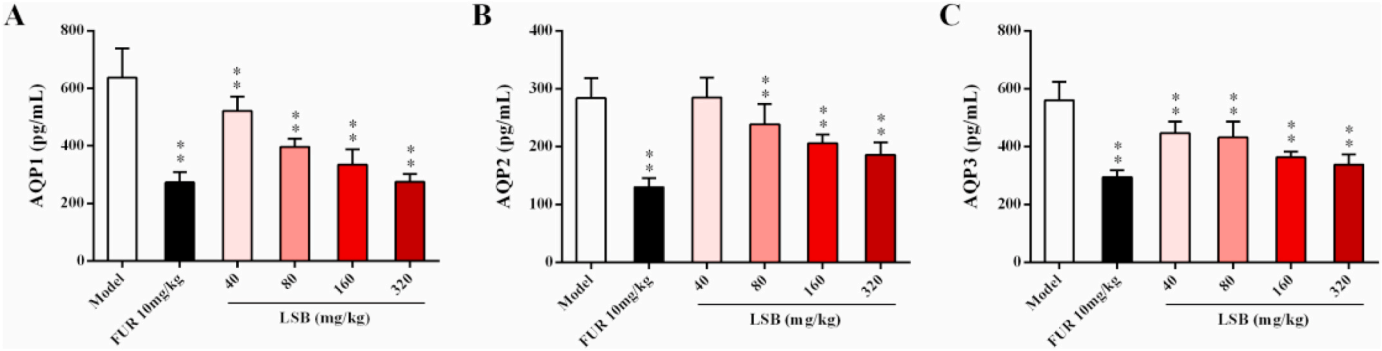

Fig. 7. Effect of LSB on serum levels of AQP1 (A), AQP2 (B), and AQP3 (C) in saline-loaded rats. Data are shown as mean ± SD (n = 8). $^{**}p < 0.01$ compared with the model group using ANOVA followed by the Dunnett's test.

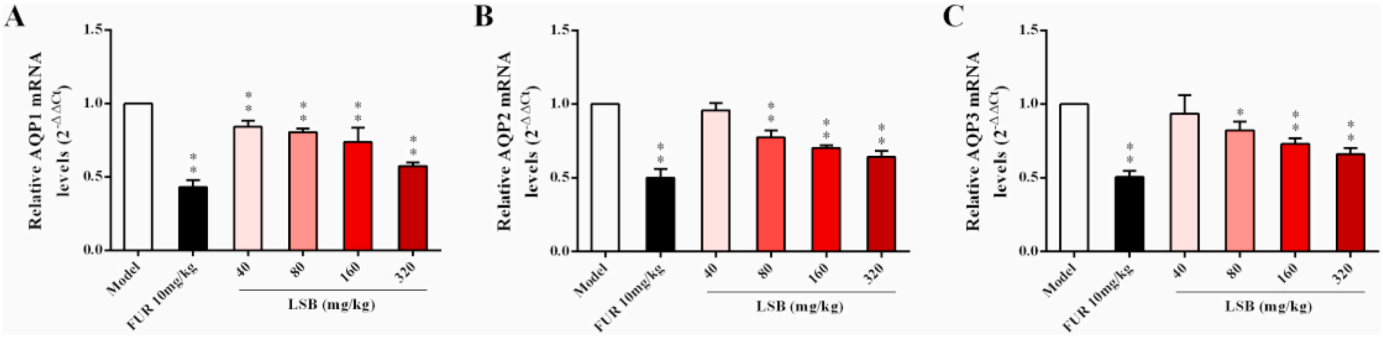

Fig. 8. Effect of LSB on the mRNA expressions of AQP1, AQP2, and AQP3 in kidney. The mRNA levels of AQP1, AQP2, and AQP3 were detected by RT-PCR. The mRNA levels of AQP1 (A), AQP2 (B), and AQP3 (C) were normalized to Model. Data are shown as mean ± SD (n = 3). $^{*}p < 0.05$ and $^{**}p < 0.01$ compared with the model group using ANOVA followed by the Dunnett's test and Mann-Whitney *U* test.

control drug of furosemide only reduced of ADH level in rats.

3.5.2. *LSB reduced serum AQP1, AQP2, and AQP3 levels*

To investigate whether LSB plays the role in AQP1, AQP2, and AQP3 excretions, we determined serum levels of these AQPs by ELISA kits in rats. As a result, the serum levels of AQP1 and AQP3 were remarkably down-regulated after treatment with any of the LSB dosages for 6 consecutive days when compared with the model group ($p < 0.01$, Fig. 7A and C), and showed a dose-dependent relationship. In addition, oral administration of 80, 160, or 320 mg/kg LSB notably decreased the AQP2 serum level in rats ($p < 0.05$ or $p < 0.01$, Fig. 7B).

3.5.3. *LSB suppressed AQP1, AQP2, and AQP3 mRNA expressions*

In continuity, the next step was to determinate the influences of LSB on the mRNA expressions of AQP1, AQP2, and AQP3 in kidney. Compared with the model group, oral administration of LSB (80–320 mg/kg) or furosemide prominently suppressed AQP1, AQP2, and AQP3 mRNA expressions in rats ($p < 0.01$, Fig. 8).

3.5.4. *LSB suppressed AQP1, AQP2, and AQP3 protein expressions*

Finally, our last step was to further evaluate the AQP1, AQP2, and AQP3 protein expressions after treatment with LSB in rats. As excepted, LSB (80–320 mg/kg) could also down-regulated the protein expressions of AQP1, AQP2, and AQP3 in rats ($p < 0.01$, Fig. 9). The results were consistent with the serum levels and mRNA expressions of AQP1, AQP2, and AQP3 in rats (Figs. 7 and 8).

Based on the above evidences, LSB possessed significantly diuretic effects via inhibiting AQP1, AQP2, and AQP3 expressions in serum and kidney tissues.

4. Discussion

Lagopsis supina has advocated as a remedy to treating various kidney disease for centuries in China (He et al., 2020). Despite LSB has an acute diuretic activity (Liu et al., 2019a), the material basis and underlying molecular mechanism are still unknown yet. In the present study, we in-depth evaluated the diuretic effects and its mechanism of LSB compared to those of furosemide, a first-line loop diuretic agent. On the one hand, LSB has a dose-dependent effects on acute and prolonged diuretic activities, and has minor effects on electrolyte excretions compared to furosemide, which significantly affected urinary electrolyte concentrations in saline-loaded rats. On the other hand, the underlying mechanisms of the diuretic caused by LSB may suppressed RAAS and AQP, as well as enhance ANP level, whereas, only suppressed ADH expression after furosemide treated. In addition, 30 phytochemicals were identified from LSB using UHPLC-qTOF-MS/MS.

In clinical practice, diuretic therapy remains the cornerstone to treating various kidney diseases, including edema, hypertension, congestive heart failure, malignant ascites effusion, stroke, and cardiovascular diseases (Cechinel-Zanchett et al., 2020; Li et al., 2020). Despite diuretic agents had been widely used to treat these diseases over several decades, some adverse effect cannot be ignored, like electrolyte disturbances, hypercalcemia, hyperglycemia, arrhythmia (Li et al., 2020; Younis et al., 2020). In this work, LSB (40–320 mg/kg) did not caused urinary Na^+ and K^+ electrolyte abnormalities, and has minor effects on urinary Cl^- and Ca^{2+} concentrations at a dosage of 320 mg/kg LSB, whereas has a prominent interference to urinary Na^+, K^+, Cl^- and Ca^{2+} concentrations after orally administration of 10 mg/kg furosemide in saline-loaded rats. Therefore, LSB may be a better diuretic agent than furosemide.

Ang II, ADH, and ALD are three hormones release from RAAS, which plays a vital role in sustaining electrolyte balance and controlling fluid

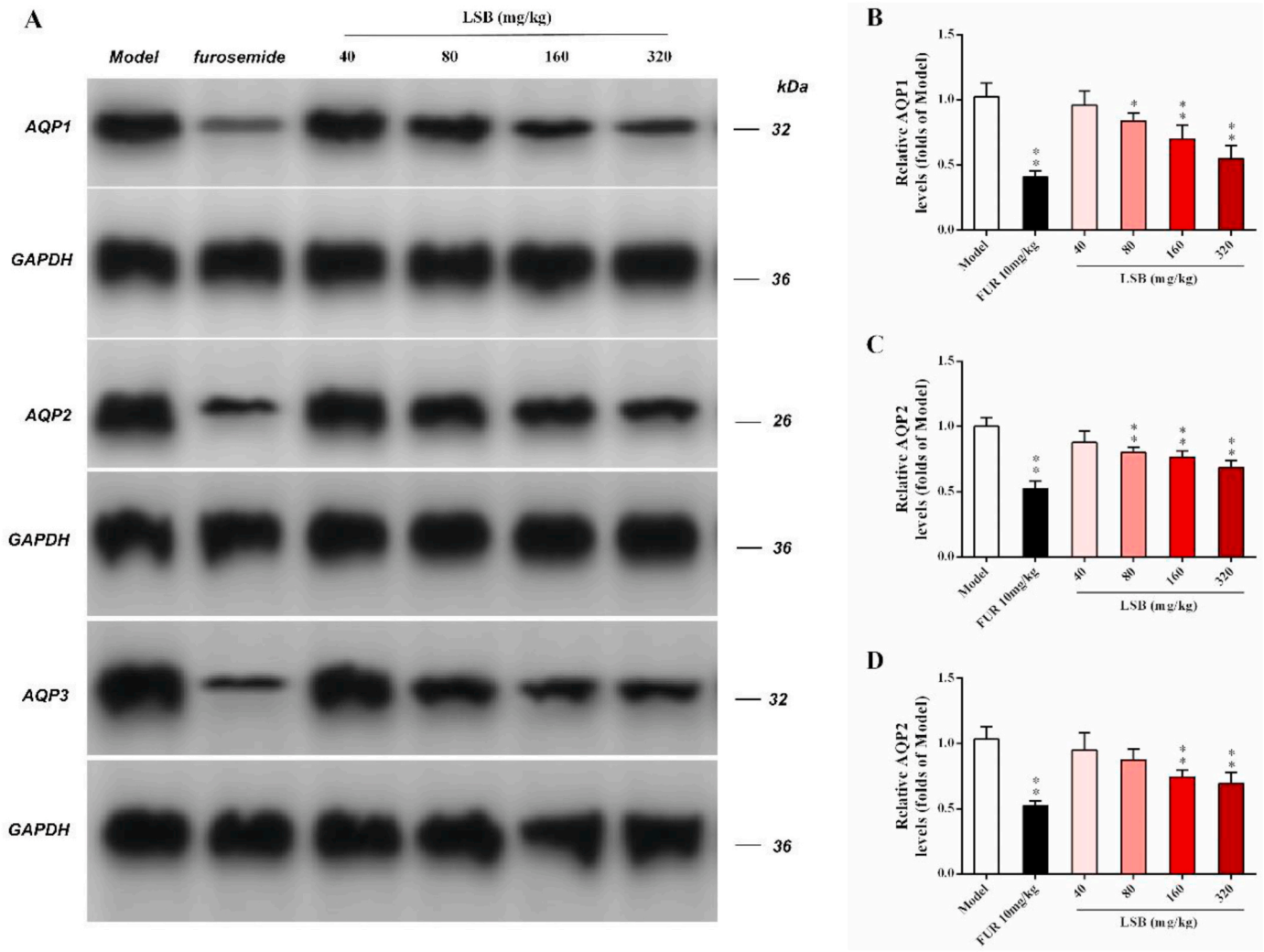

Fig. 9. The levels of AQP1, AQP2, and AQP3 protein expression from different groups was detected by Western blot assay, and representative bands were shown in (A). The levels of AQP1(B), AQP2 (C), and AQP3 (D) were normalized to model group. Data are shown as mean ± SD (n = 3). *$p < 0.05$ and **$p < 0.01$ compared with the model group using ANOVA followed by the Dunnett's test.

homeostasis by regulating the nephron (He et al., 2019a; Lou et al., 2018; Kumar et al., 2016; Liu et al., 2019a). On the side, ANP is a hormone derivate from heart, not only plays a dominant role in maintaining body fluid and electrolyte balance, but also inhibiting the RAAS activation (Lou et al., 2018; Kumar et al., 2016; Liu et al., 2019a). Thus, suppress RAAS and elevate ANP appear to be an effective strategy to promote urinary excretion volume. Recent our previous study indicated that the ethanol crude extract and its four soluble fractions from L. supina showed potential diuretic activity in saline-loaded rats (He et al., 2019a; Liu et al., 2019a). In this work, LSB (80–320 mg/kg) observably suppressed RAAS activation, including decreased serum levels of Ang II, ADH, and ALD in rats, and prominently increased serum level of ANP. In contrast, only decreased serum level of ADH after furosemide-treated. The results showed that LSB possessed diuretic effect through multiple targets, whereas, only ADH was related to furosemide.

AQP1, AQP2, and AQP3 are three membrane proteins, closely related to water transport, and play a pivotal role in the urinary reabsorption and excretion (He et al., 2019a; Kortenoeven and Fenton, 2014; Xing et al., 2014). In this experiment, LSB significantly down-regulated serum AQP1, AQP2, and AQP3 excretions in rats compared to the model group. In continuously, the mRNA and protein expressions of three above mentioned membrane proteins were remarkably suppressed after treatment with LSB in a dose-dependent manner compared to the model group in rats. Therefore, we demonstrated that LSB may exerts its diuretic activity by modulating AQP1, AQP2, and AQP3 expressions in rats, which consistent with previous study (He et al., 2019a).

Previous phytochemical studies have found that diterpenoids, flavonoids, and phenylpropanoids are the major phytochemical constituents of *L. supina* (He et al., 2020; Yang and He, 2020), and some diterpenoids showed potential anti-inflammatory against BV-2 cells *in vitro* (Li et al., 2014). Moreover, phenylpropanoids and flavonoids exert diuretic effect in rats were reported in previous studies (Ansari et al., 2018; Bhanuvalli et al., 2020; Prando et al., 2016; Souza et al., 2017). In the present work, 11 phenylpropanoids, 9 flavonoids, 5 monoterpenoids, 2 diterpenoids, and 3 others were identified from LSB based on UHPLC-qTOF-MS/MS. Among them, caffeic acid (peak 12, 10 mg/kg, p.o.) possessed significantly increased urinary excretion volume in saline-loaded rats when compared with the vehicle-treated rats (Moser et al., 2020). Furthermore, oral administration of luteolin (peak 25, 3 mg/kg) showed prominent diuretic effect in normotensive and hypertensive rats (Boeing et al., 2017). Additionally, numerous studies indicated that phenylpropanoids and flavonoids exert diuretic effect in rats (Ansari et al., 2018; Bhanuvalli et al., 2020; Prando et al., 2016; Souza et al., 2017). Consequently, phenylpropanoids and flavonoids may be responsible for the major active constituents of LSB exerts diuretic effects in rats; however, further studies are needed to isolate and identify

the bio-constituents directly related to diuretic effects and its probable mechanism in vivo and in vitro of this crude extract.

5. Conclusions

In summary, this study demonstrated that LSB obtained from *L. supina* has significant acute and prolonged diuretic effects *via* inhibiting the AQP and RAAS pathways in saline-loaded rats, and supports the traditional folk use of this plant. LSB might be a potential diuretic agent to treat kidney diseases with minor effects on electrolyte excretions in clinical practice.

Author contributions

Junwei He and Li Yang contributed to study design, experiments, data interpretation, and wrote the manuscript. Junwei He and Zhongwei He revised the manuscript.

Declaration of competing interest

All authors declare that they have no conflict of interest.

Acknowledgments

This work was financially supported by grants from the Standard Revision Research Project of National Pharmaceutical Council (no. 2018Z092), and the Jiangxi University of Traditional Chinese Medicine (nos. JXSYLXK-ZHYA0031, 2016RC001, and JXXT2017008).

References

Ansari, M.N., Ganaie, M.A., Khan, T.H., 2018. Evaluation of the diuretic potentials of naringenin in hypercholesterolemic rats. Trop. J. Pharmaceut. Res. 17, 239–244.

Angeloni, S., Nzekoue, F.K., Navarini, L., Sagratini, G., Torregiani, E., Vittori, S., Caprioli, G., 2020. An analytical method for the simultaneous quantification of 30 bioactive compounds in spent coffee ground by HPLC-MS/MS. J. Mass Spectrom. 55, e4519.

Bhanuvalli, R.S., Lotha, R., Sivasubramanian, A., 2020. Phenylpropanoid rich extract of edible plant *Halosacia indica* exert diuretic, analgesic, and anti-inflammatory activity on Wistar albino rats. Nat. Prod. Res. 34, 1616–1620.

Boeing, T., Silva, L.M., Mariott, M., Andrade, S.F., Souza, P., 2017. Diuretic and natriuretic effect of luteolin in normotensive and hypertensive rats: role of muscarinic acetylcholine receptors. Pharmacol. Rep. 69, 1121–1124.

Cechinel-Zanchett, C.C., Mariano, L.N.B., Boeing, T., Costa, J.C., Silva, L.M.D., Bastos, J. K., Cechinel-Filho, V., Souza, P., 2020. Diuretic and rental protective effect of kaempferol 3-*O*-alpha-L-rhamnoside (Afzelin) in normotensive and hypertensive rats. J. Nat. Prod. 83, 1980–1989.

He, J.W., Zeng, L.B., Wei, R.R., Zhong, G.Y., Zhu, Y.Y., Xu, T.T., Yang, L., 2019a. *Lagopsis supina* exerts its diuretic effect via inhibition of aquaporin-1, 2 and 3 expression in a rat model of traumatic blood stasis. J. Ethanopharmacol. 231, 446–452.

He, D., Huang, X.L., Chen, L., Liang, X.J., Zhu, L.H., Zhang, S.H., 2019b. Study on substance basis of compound *Smilacis chinae* rhizome in vitro by HPLC-Q-TOF-MS. Chin. J. Inform. Trad. Chin. Med. 26, 68–73.

He, J.W., Yang, L., Xu, T.T., Zhong, G.Y., 2020. Comparison of clinal application and modern research of *Lagopsis supina* used in different ethnic medicine culture. Chin. Tradit. Herb. Drugs 51, 4576–4585.

Jiménez-Sánchez, C., Lozano-Sánchez, J., Rodríguez-Pérez, C., Segura-Carretero, A., Fernández-Gutiérrez, A., 2016. Comprehensive, untargeted, and qualitative RP-HPLC-ESI-QTOF/MS^2 metabolite profiling of green asparagus (*Asparagus officinalis*). J. Food Compos. Anal. 46, 78–87.

Kortenoeven, M.L.A., Fenton, R.A., 2014. Renal aquaporins and water balance disorders. BBA-Gen. Subj. 1840, 1533–1549.

Kumar, K., Sharma, S., Vashishtha, V., Bhardwaj, P., Kumar, A., Barhwal, K., Hota, S.K., Malairaman, U., Singh, B., 2016. *Terminalia arjuna* bark extract improves diuresis and attenuates acute hypobaric hypoxia induced cerebral vascular leakage. J. Ethanopharmacol. 180, 43–53.

Li, H., Li, M.M., Su, S.Q., Sun, J., Gu, Y.F., Zeng, K.W., Zhang, Q., Zhao, Y.F., Ferreira, D., Zjawiony, J.K., Li, J., Tu, P.F., 2014. Anti-inflammatory labdane diterpenoids from *Lagopsis supina*. J. Nat. Prod. 77, 1047–1053.

Li, M., Zhao, Y., Zhang, S., Xu, Y., Wang, S.Y., Li, B.W., Ran, J.H., Li, R.T., Yang, B.X., 2020. A thienopyridine, CB-20, exerts diuretic activity by inhibiting urea transporters. Acta Pharmacol. Sin. 41, 65–72.

Liu, Z.Y., Yang, L., Li, R.X., Wei, R.R., Luo, X.Q., Xu, T.T., Huang, Y., Mu, Z.J., He, J.W., 2019a. Diuretic and anti-diuretic activities of ethanol extract and fractions of *Lagopsis supina* in normal rats. BioMed Res. Int. 2019, 6927374.

Liu, M., He, M.Z., Gao, H.W., Guo, S., Jia, J., Ouyang, H., Feng, Y.L., Yang, S.L., 2019b. Strategy for rapid screening of antioxidant and anti-inflammatory active ingredients in *Fynura procumbens* (Lour.) Merr. based on UHPLC-Q-TOF-MS/MS and characteristic ion filtration. Biomed. Chromatogr. 33, e4635.

Liu, X.C., Fan, X.Y., Wang, X., Liu, R.N., Meng, C.F., Wang, C.Y., 2019c. Structural characterization and screening of chemical markers of flavonoids in *Lysimachiae* herba and *desmodii styracifolii* herba by ultra high-performance liquid chromatography quadrupole time-of-flight tandem mass spectrometry based metabolomics approach. J. Pharmaceut. Biomed. 171, 52–64.

Lou, J.W., Cao, L.L., Zhang, Q., Jiang, D.J., Yao, W.F., Bao, B.H., Cao, Y.D., Tang, Y.P., Zhang, L., Wang, K., Dai, G.C., 2018. The toxicity and efficacy evaluation of different fractions of kansui frybaked with vinegar on walker-256 tumor-bearing malignant ascites effusion rats and normal rats. J. Ethanopharmacol. 219, 257–268.

Moser, J.C., Cechinel-Zanchett, C.C., Mariano, L.N.B., Boeing, T., Silva, L.M., Souza, P., 2020. Diuretic, natriuretic and Ca^{2+}-sparing effects induced by rosmarinic and caffeic acids in rats. Rev. Bras. Farmacogn. 30, 588–592.

Prando, T.B.L., Barboza, L.N., Araújo, V.O., Gasparotto, F.M., Souza, L.M., Lourenco, E.L. B., Junior, A.G., 2016. Involvement of bradykinin B2 and muscarinic receptors in the prolonged diuretic and antihypertensive properties of *Echinodorus grandifloras* (Cham. & Schltdl.) Micheli. Phytomedicine 23, 1249–1258.

Souza, P., Silva, L.M., Boeing, T., Somensi, L.B., Cechinel-Zanchett, C.C., Campos, A., Krueger, C.M.A., Bastos, J.K., Cechinel-Filho, V., Andrade, S.F., 2017. Influence of prostanoids in the diuretic and natriuretic effects of extracts and kaempferitrin from *Bauhinia forficate* Link leaves in rats. Phytother Res. 31, 1521–1528.

Wu, Y., Qiu, Z.H., Bai, W.J., Dong, Z.J., 2017. Rapid analysis of chemical constituents in Xuanmai Ganjie granules by UHPLC-Q-TOF-MS. Chin. J. Exp. Tradit. Med. Form. 23, 70–76.

Xing, L., Wen, J.G., Frøkiær, J., Djurhuus, J.C., Nørregaard, R., 2014. Ontogeny of the mammalian kidney: expression of aquaporins 1, 2, 3, and 4. World J. Pediatr. 10, 306–312.

Yang, L., He, J.W., 2019. *Hosta plantaginea* (Lam.) Aschers (Yuzan): an overview on its botany, traditional use, phytochemistry, quality control and pharmacology. RSC Adv. 9, 35050–35058.

Yang, L., Liu, R.H., He, J.W., 2019. Rapid analysis of the chemical compositions in *Semiliquidambar cathayensis* roots by ultra-high-performance liquid chromatography and quadrupole time-of-flight tandem mass spectrometry. Molecules 24, 4098.

Yang, L., He, J.W., 2020. *Lagopsis supina* extract and its fractions exert prophylactic effects against blood stasis in rats via anti-coagulation, anti-platelet activation and anti-fibrinolysis and chemical characterization by UHPLC-qTOF-MS/MS. Biomed. Pharmacother. 132, 110899.

Yang, L., Liu, S.Z., Liu, R.H., He, J.W., 2020a. Bioassay-guided isolation of cyclooxygenase-2 inhibitory and antioxidant phenylpropanoid derivatives from the roots of *Dendropanax dentiger*. Bioorg. Chem. 104, 104211.

Yang, L., Lin, Y.M., He, Z.W., Zhang, T.F., Li, Y., Xie, X.T., Wu, Y.F., He, J.W., 2020b. Hostaflavanol A, a new anti-inflammatory and antioxidant activities flavanol from the flowers of *Hosta plantaginea*. Med. Chem. Res. 29, 426–430.

Yang, L., Zhu, Y.Y., He, Z.W., Zhang, T.F., Xiao, Z.X., Xu, R.L., He, J.W., 2020c. Plantanone D, a new rare methyl-flavonoid from the flowers of *Hosta plantaginea* with anti-inflammatory and antioxidant activities. Nat. Prod. Res. online. https://doi.org/10.1080/14786419.2020.1713121.

Yang, L., He, J.W., 2021. Traditional uses, phytochemistry, pharmacology and toxicological aspects of the genus *Hosta* (Liliaceae): a comprehensive review. J. Ethanopharmacol. 265, 113323.

Younis, W., Schini-kerth, V.B., Silva, D.B., Junior, A.G., Bukhari, I.A., Assiri, A.M., 2020. Role of the NO/cGMP pathway and renin-angiotensin system in the hypotensive and diuretic effects of aqueous fraction from *Crataegus songarica* K. Koch. J. Ethanopharmacol. 249, 112400.

Zhang, Q.Q., Dong, X., Liu, X.G., Gao, W., Li, P., Yang, H., 2016. Rapid separation and identification of multiple constituents in Danhong Injection by ultra-high performance liquid chromatography coupled to electrospray ionization quadrupole time-of-flight tandem mass spectrometry. Chin. J. Nat. Med. 14, 147–160.

Zhou, F., Lin, M.S., Li, R., Zhang, C.R., Zhao, L., Lin, D.S., Cao, K., 2020. Analysis of chemical constituents in baihe dihuangtang by UHPLC-Q-TOF-MS. Chin. J. Exp. Tradit. Med. Form. 26, 15–22.